Measurements in support of wind farm simulations and power forecasts: The Crop/Wind-energy Experiments (CWEX)

E S Takle[1,5], D A Rajewski[1], J K Lundquist[2], W A Gallus, Jr.[3], and A Sharma[4]

[1] Agronomy Department, Iowa State University, Ames, IA 50011 USA
[2] Department of Atmospheric and Oceanic Sciences, University of Colorado, Boulder, CO, 80309 USA and National Renewable Energy Laboratory, Golden, CO
[3] Geological and Atmospheric Sciences Department, Iowa State University, Ames, IA 50011 USA
[4] Aerospace Engineering Department, Iowa State University, Ames, IA 50011 USA
Email: gstakle@iastate.edu

Abstract. The Midwest US currently is experiencing a large build-out of wind turbines in areas where the nocturnal low-level jet (NLLJ) is a prominent and frequently occurring feature. We describe shear characteristics of the NLLJ and their influence on wind power production. Reports of individual turbine power production and concurrent measurements of near-surface thermal stratification are used to turbine wake interactions and turbine interaction with the overlying atmosphere. Progress in forecasting conditions such as wind ramps and shear are discussed. Finally, the pressure perturbation introduced by a line of turbines produces surface flow convergence that may create a vertical velocity and hence a mesoscale influence on cloud formation by a wind farm.

1. Introduction

During 2012, the state of Iowa generated almost 25% of all its electricity from wind turbines [1]. Its largest electric utility will be generating 39% of its base load from wind in 2015. Continued expansion of wind energy in Iowa calls for a better understanding of wind-farm interactions with the atmospheric boundary layer and wind-farm/wind-farm interactions. We describe field measurements, numerical simulations, and forecast-model research for improving understanding of wind farm characteristics and identifying opportunities for improving day-ahead wind power forecasts.

In 2010 Iowa State University launched its first field campaign to study meteorological and aerodynamic conditions in operating wind farms. Eighty-six percent of the Iowa landscape is devoted to cropland, so our initial research focused on the interactions of turbines with crops and was named the Crop/Wind-energy EXperiment (CWEX). CWEX has continued as an annual warm-season measurement campaign with increased emphasis on the aerodynamics of wind farms, including research on wind farm simulation and wind power forecasts [2]. CWEX field campaigns in summers 2010 and 2011 included surface flux measurements and lidar observations in a 200-turbine utility scale wind farm in central Iowa having 1.5 MW turbines with 80-m towers and 37-m blades. Site description, measurement network and results are available in [2]. A second Iowa wind farm, having 171 1.6 MW turbines and two nearby meteorological towers, serves as a field site for improving wind farm power forecasts. These two wind farms, separated by about 100 km, are used to explore the occurrences of sequential and synchronous ramp events. The high wind-resource region of the US Great Plains and Midwest has a high frequency occurrence of nocturnal low-level jets (NLLJs) as described in the next section.

2. Impact of the Nocturnal Low-Level Jet on shear across the turbine rotor

Stably stratified nighttime flow over flat terrain has long been the subject of experimental and numerical studies. Of particular interest of early studies was the need to explain the large supergeostrophic wind maximum, often referred to as the nocturnal low-level jet (NLLJ), which frequently is observed late at night in the lowest few hundred meters in the earth's atmosphere Bonner

[5] To whom correspondence should be addressed

[3]. Blackadar [4] explained the NLLJ in terms of an inertial (induced by the Coriolis force) oscillation of the wind vector after collapse of mechanically generated day-time turbulence in the surface layer. This phenomenon is different from the Great Plains Low-Level Jet (GPLLJ) that has its origin in the east-west temperature gradient from the Rocky Mountains to the Missouri River and has a much higher elevation, although both jets are accelerated by the inertial oscillation.

Delage [5] and Thorpe and Guymer [6] provided numerical models that captured the essential features of the NLLJ in barotropic flow. Zeman [7] extended early models to consider the effects of geostrophic wind shear (baroclinicity) and sloped terrain on the vertical properties of the boundary-layer winds. He concluded that small values of baroclinicity increase the ageostrophic flow without significantly altering the rate of destruction of the thermal stratification and thereby increase the magnitude of the jet maximum. Higher values of geostrophic wind shear, however, hinder the morning destruction of the nocturnal boundary layer by increased turbulent downward transport of momentum from above the jet. This elevates the level of jet speed maximum but reduces its lifetime. Russell and Takle [8] extended the work of Zeman [7] by use of a multilevel model that explicitly represented vertical gradients of the geostrophic wind. In general agreement with previous studies, they found the jet speed maximum to be over 40% higher than geostrophic winds above the jet. For flat terrain and low surface roughness, the height of the maximum was about 60 m above ground level. Their modeling study showed that very weak ageostrophic wind shear (0.0005 s^{-1}) increases the jet maximum by 10% and extends its lifetime by half an hour, but that values of 0.004 s^{-1} reduced the magnitude of the maximum, raised its height, and shortened its lifetime.

Observations and modeling studies clearly show the relation of stable boundary layer stratification to strong vertical shear in the horizontal wind [9, 10] in the lowest few 100 m. Figure 1 shows wind speed, wind direction, temperature, and Richardson number observed from an Iowa 200-m tower.

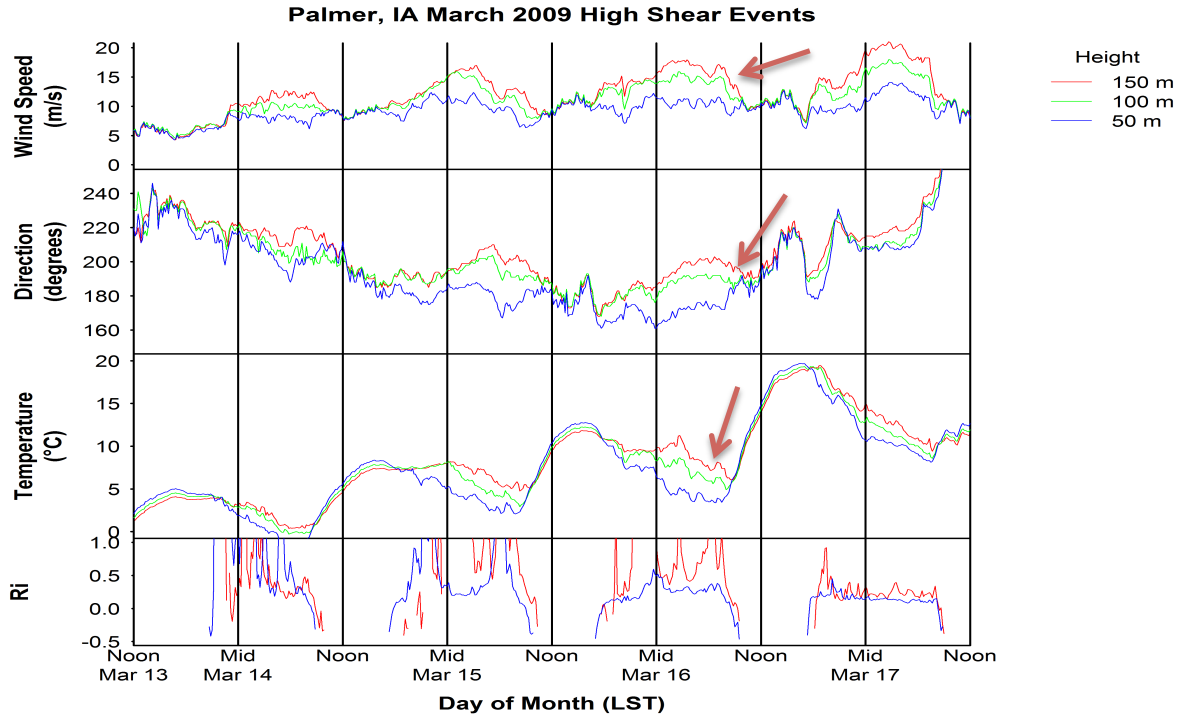

Figure 1: Wind speed, wind direction, temperature, and Richardson number observed from a 200-m tower in northwest Iowa for 13-17 March 2009. Arrows mark the nocturnal period of high shear in wind speed and direction and large temperature gradient between 50 m and 150 m.

Of particular note is the abrupt reversal of the vertical gradient of temperature at about 1800 LST (6 PM local time) when the boundary layer stabilizes, quenching the daytime turbulence and initiating a low-turbulence laminar flow regime. The wind speed profile responds to this collapse of frictional drag forces by accelerating the flow to magnitudes that increase with height. This is clearly revealed

by comparison of the actual observed winds with the geostrophic wind (Vg), which is calculated from the horizontal pressure gradient that drives the flow. During daytime periods (see highlighted daytime low-shear period) the turbulent frictional forces create a drag on the flow that reduces the actual wind speed to magnitudes below Vg. But with the collapse of frictional forces near sunset, the loss of drag forces creates a force imbalance that accelerates the flow, more-so at higher elevations where the reduction of the frictional component was larger (see highlighted nighttime high-shear period). The actual flow exceeds the geostrophic value, clearly revealing the lower portion of the NLLJ. The peak speed of the jet is above the top of the 200-m tower during this four-day period.

3. Lidar measurements in a region of strong Nocturnal Low-Level Jets

As part of the CWEX-11 campaign, two vertically profiling Doppler wind lidars (Windcube V1) described in [11] were deployed within the CWEX wind farm. Except during a brief intercomparison period, one lidar (CU1) was located approximately 165 m south (2*D*) of a row of six turbines in an west-east line; the second lidar (CU2) was located 250 m north (3*D*) of the same wind turbine line. The lidar deployment is discussed in detail in [12].

CWEX-11 frequently featured southerly flow, particularly during nocturnal conditions, so that the southerly (or "upwind") lidar can quantify the behavior of lower regions of the NLLJ. The night of 9 July 2011 presents a representative case (Figs 2, 3). The jet begins to form relatively early in the evening, with speeds of 9 m s^{-1} (compared to daytime flow of approximately 5 m s^{-1} at all altitudes observed by the lidar, not shown). The maximum wind speed observed by the lidar occurs twice, during two pulsating events at 0200 LST and again near 0530 LST. This pulsating behavior is often observed with nocturnal NLLJ [13, 14]. The wind direction time-height cross-sections confirm that daytime conditions tend to not include much change of wind direction with height, but the times of peak NLLJ wind speed also include significant wind veer.

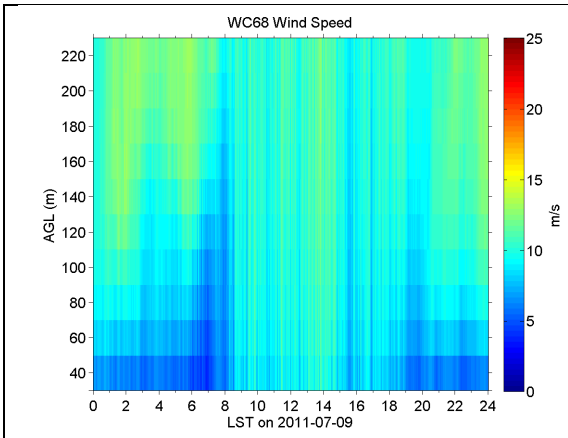

Figure 2: Time-height cross-section of horizontal wind speed from the southerly lidar on 9 July 2011. The maximum wind speed of the NLLJ is at least 14 m s^{-1}, forming soon after sunset and dissipating by 800 LST.

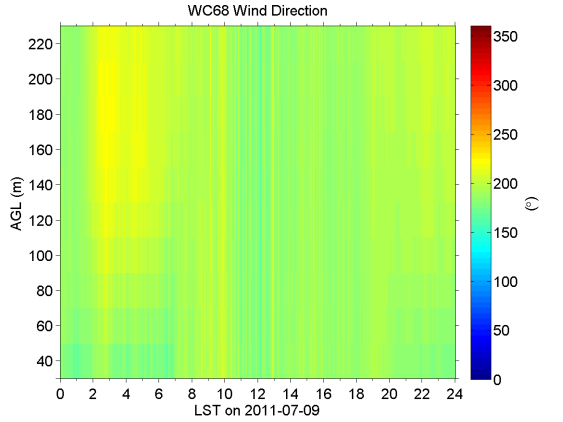

Figure 3: Time-height cross-section of horizontal wind direction from the southerly lidar on 9 July 2011. During the NLLJ conditions, at least 35 degrees of wind veer exists between the 40-m level the 180-m level.

4. Potential influence of high-shear on wind farm power production

For CWEX-10, four surface flux stations, designated NLAE 1-4 in Fig. 4, were provided by the National Laboratory for Agriculture and the Environment. The upwind flux tower in CWEX-10 was placed about 4.5 D south of the southern line of turbines (X-A-B-C-D-E in Fig. 4) to document the undisturbed flow of the prevailing southerly winds. The second and third flux towers were positioned about 2.5 D and 17 D north of the south turbine line, respectively, and a fourth station was placed north of the north turbine line at about 35 D downwind of the south turbine line. In CWEX-11 four flux stations were provided by the National Center for Atmospheric Research (NCAR). The upwind

reference tower (NCAR 1) was placed 2.0 D south of the south turbine line, and downwind flux towers (NCAR 2-4) were placed 3.5 D, 9 D, and 14 D, respectively, north of the south turbine line. Two flux towers provided by Iowa State University (ISU 1 and ISU 2) were placed north and south of the midpoint between turbines A and B, at 2.0 D upwind and 3.5 D downwind, respectively.

We calculate normalized power difference from a reference turbine (X in Fig. 4) within the south turbine line and identify daytime and nighttime variations in power across multiple turbines in both lines of turbines. Differences are categorized by upwind station surface stability and the reference turbine nacelle yaw direction. Three ambient stability categories are defined as: neutral ($|z/L|<0.05$), stable ($z/L>0.05$) and unstable ($z/L<-0.05$), where z is the height of the sonic

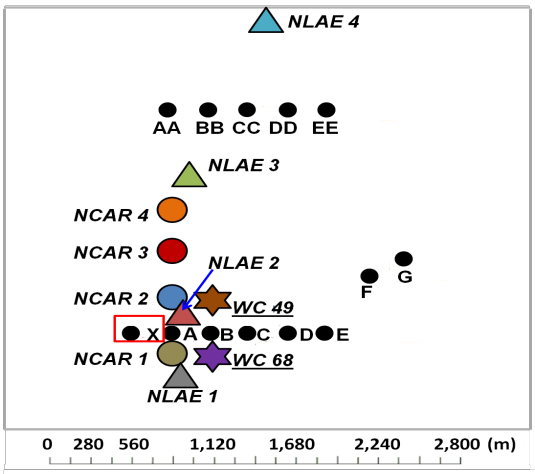

Figure 4. Locations of surface flux stations (NCAR 1, 2, 3, 4) and NLAE (1, 2, 3, 4) and wind profiling lidars (WC49, WC68) in relation to turbines (X, A-G, and AA-EE) for the CWEX-10/11measurement campaigns. The reference turbine, denoted by X boxed in red, is used for normalizing power differences. Turbine lines X-A-B-C-D-E and AA…EE are east west line, with AA…EE being the north line.

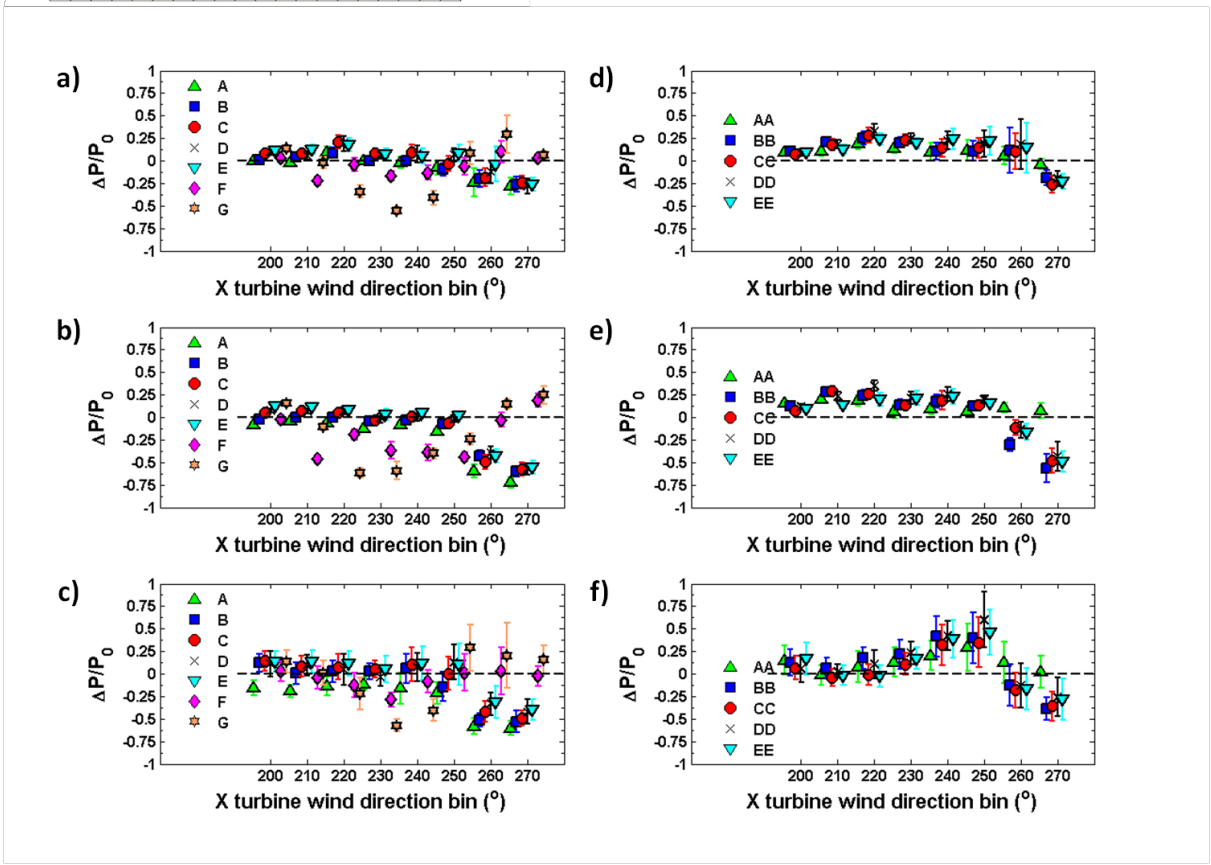

Figure 5. Means and 95% confidence intervals of the normalized power differences from a reference turbine (X) and response to changes in the reference wind direction for the south lines of turbines in a) neutral, b) stable, and c) unstable conditions and for the north line of turbines in d) neutral, e) stable, and f) unstable conditions.

measurement and L is the Monin-Obukhov length (see [2] for details). We plot data for a subset of wind directions from 220° to 270° to illustrate the spatial variability in the power difference and illustrate the variation of the differences with the 95% confidence intervals. In Fig. 5 we plot normalized power at the south line of turbines for (a) neutral, (b) stable, and (c) unstable conditions and for the north line for (d) neutral, (e) stable, and (f) unstable conditions. Winds from S-SSW indicate small to negligible departure from the reference power in both day and night periods. The two turbines (F and G) northeast of the first turbine line show a strong influence on power production for directions from SW to WSW in all stability conditions. However, for westerly winds there is a slight increase in production for the F and G turbines, while concurrently power is reduced by 25-60% for turbines within the south turbine line as multiple wakes are impacting successive turbines within the line (Figs 5 a-c). We interpret the power enhancement at F and G to be due to mixing down of higher speed air from above under high-shear conditions by the edge of the reference turbine wake as it is passing to the southeast of the F and G turbines. Among variations within the first line for near-westerly wind, the turbine closest to the reference station has the largest drop in power for stable and unstable conditions (50-75%) and the turbine farthest downwind of the reference turbine indicates some speed recovery (i.e. power deficit weakened by 25%). The power differences are most variable in unstable conditions for all turbines, and the multiple-turbine reductions in power are least when the flow is near neutral.

For the north line of turbines we observe a nearly 25% power enhancement in both neutral and stable conditions for winds from the SW (Figs. 5 d, e). The characteristics of the NLLJ and the power differences between the two turbine lines in stable, high-shear conditions are linked to the terrain surrounding the wind farm. The combination of 8-10-m higher terrain at the north line and the larger terrain gradient for southwesterly fetch are responsible for the 25% power increase. In SSW winds, turbines AA, BB, CC, and DD have 10-15% higher power than turbine EE in the same line. The power drop for EE is related to the wakes from the X, A, and B turbines.

For unstable conditions the power differences among turbines is negligible for near southerly to southwesterly winds (Fig. 5 f) presumably because the wakes from the south line are diluted by ambient turbulence. For winds from the WSW power is enhanced by 25-60% within the north line of turbines and we posit three factors: (1) higher terrain at the north line of turbines, (2) daytime fluxes from land-surface heterogeneities, and (3) high shear within the turbine layer during the decay of the NLLJ may contribute to spatial variations in hub height wind speed [3]. For westerly winds in near neutral flow turbines BB, CC, DD, and EE reported a 20-30% power reduction. Turbine BB experienced the largest power depletion (40-60%) in both stable and unstable conditions, whereas the turbine farthest downwind (EE) has about a 10-20% recovery from the maximum drop.

5. Improvements in wind speed forecasting by use of ensembles

Improvements in the accuracy of forecasts of wind at turbine height are critical to improve performance at wind farms. Unfortunately, until recently meteorologists generally focused their attention for lower tropospheric winds to the 10 m elevation, the standard level for reporting surface winds, and relatively little work has been done to understand the errors in wind forecasts at heights more typical of wind turbines. Flow at turbine height can behave much differently from that at 10 m elevation, as the turbines will often be above the layer where friction greatly impacts winds under stable conditions, which occur frequently at night and occasionally during daytime as well.

Some prior research has been performed on winds at turbine height. Wood [15] and Ayotte et al [16] examined flow in the western United States, but since this was an area of complex terrain, the findings may not be applicable in Iowa where boundary layer stratification, low-level jets (LLJs), and changing surface conditions are likely to be the dominant factors providing uncertainty in short-term forecasts at 80 m. Deppe et al. [17] examined forecasting of winds at turbine height for day 2 for a wind farm in Iowa using several different ensemble approaches. That study found systematic problems in all six different planetary boundary layer parameterizations tested that are commonly

used in the Weather Research and Forecasting (WRF) model, with insufficient spread among the different schemes. However, bias corrections applied as a post-processing technique to an ensemble that consisted of mixed initial and lateral boundary conditions, mixed planetary boundary layer schemes, and different initialization times were able to produce a statistically significant improvement in mean absolute errors for day-ahead wind speed forecasts at 80 m.

It is important to note, however, that power generation is affected by several factors that operate on smaller scales than those typically resolved by models like the WRF, and thus forecasts of parameters besides wind speed may be necessary. Turbine interaction will be a function of wind direction and thermodynamic stability. In addition, as shown in Fig. 1, intense vertical shears can develop near turbine height. Accurate prediction of these vertical shears (both directional and speed changes) is needed since the shears put stress on turbine blades (speed shear) and change the angle of attack for blades at the top of the rotation from those at the bottom (directional shear). The strongest shears often develop on nights with the strongest temperature inversions, and it is in these very stable conditions that commonly used planetary boundary layer schemes may produce the biggest errors. Evidence of problems during low-level jet events can be seen in Hu et al. [18] which offers a thorough review of some of the problems impacting forecasting of winds and shear near the ground. Research by our group reported elsewhere [19] focuses on improving the boundary-layer parameterization in WRF by including turbulence anisotropies under highly stable stratification.

As difficult as it is to make accurate day 2 forecasts, forecasts of ramp events, rapid changes in wind speed that lead to extreme changes in wind power output, are even more challenging. These ramps can be extremely costly to energy companies because they may cause blackouts and overload the grid [20]. Greaves et al. [21] found that ramp events were captured less than 36% of the time by a private forecast company forecasting for six wind farms in the United States. Deppe et al. [17] found for an Iowa wind farm that over the course of a year, an average of roughly 1 ramp up and 1 ramp down occurred each day, and every planetary boundary layer scheme used in the WRF model underpredicted the number of ramps. Even allowing for time errors of up to 6 hours for ramp prediction, threat scores for all schemes tended to average around 0.2 to 0.3 for day 1 and day 2 forecasts. More encouraging may be the finding of Showers Walton et al. [22] who found for an 18 month period that 40% of the ramps at a central Iowa wind farm occurred within 6 hours of a ramp at another farm roughly 160 km west, implying the potential to improve short-term forecasting if wind data at turbine height are available to forecasters. The spatially consistent ramps tended to occur when a large synoptic pressure gradient existed or a front was involved. Deppe et al. [17] and Showers Walton et al. [22] both found that there are numerous possible causes for ramps, and a rather large fraction for which it is difficult to assign a cause from standard observations, suggesting additional study with enhanced observations might improve the ability to forecast these events. Finally, more recently [23] showed that ramp events can exhibit large spatial variability on very small scales, with roughly 75% of all ramps within a central Iowa wind farm not occurring at all turbines examined within the farm within a reasonable time interval. The most common scenario was for ramps to be experienced at some turbines but not others, although in a few cases, a ramp up occurred at one turbine while a ramp down occurred at another in the same section of the wind farm at roughly the same time. An especially fine network of observations would be necessary to better understand ramp behavior within a wind farm.

6. Wind farm aerodynamics model validation with CWEX field data

A wind farm aerodynamics model that solves the Reynolds Averaged Navier-Stokes (RANS) equations with a generalized actuator disk representation for turbines has been developed. This model has been validated against 1-D momentum theory and against single-turbine measured data [24]. We apply this model to investigate the phenomenon of surface flow convergence in wind farms observed in the CWEX data. It has been observed that, near the ground, turbine rows align the flow coming at an angle, with the direction perpendicular to the first line of turbines seen by the flow (see Fig. 6). Surface flow convergence can have important meteorological implications. If a large-scale wind farm causes flow in the lowest 80 m to converge, conservation of mass requires a positive vertical velocity

over top of the wind farm. An enhancement of ambient vertical velocity would create preferential conditions for cloud formation and possible triggering of rainfall.

A plausible explanation for surface flow convergence was provided by [24]. Across a turbine rotor, static pressure drops sharply but then subsequently recovers to its free-stream value far downstream of the rotor. In an array of turbines, this pressure recovery may not completely occur before the next downstream turbine further decreases the pressure. In a large array of turbines therefore, static pressure continues to drop through the array. This drop in pressure creates a pressure gradient along the direction perpendicular to the upwind line of turbines (high upstream and low downstream) as shown in Fig. 7. The flow is driven in the direction of decreasing pressure, causing flow convergence.

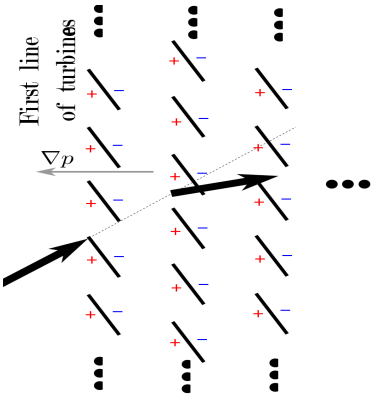

Figure 6: A schematic illustrating flow convergence due to turbines in a wind farm.

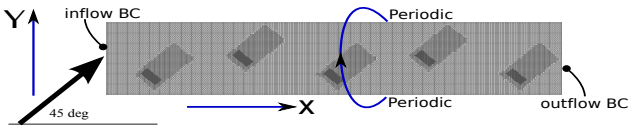

Figure 7: Hypothetical wind farm simulation setup.

A hypothetical farm is first simulated with periodic boundary conditions (Fig. 7). Each line of turbines (along the Y direction) therefore has an infinite number of turbines. Inflow is uniform and at 45° to the X axis (which is perpendicular to the direction of the upwind line of turbines). Figure 7 shows contours of pressure and local flow angle (w.r.t. the X direction) on the ground and the average (in the Y direction) pressure and flow angle variation with downstream distance. The flow angle drops successively behind each turbine due to the pressure differential imposed the turbines. A net flow angle deviation of about 10° is observed.

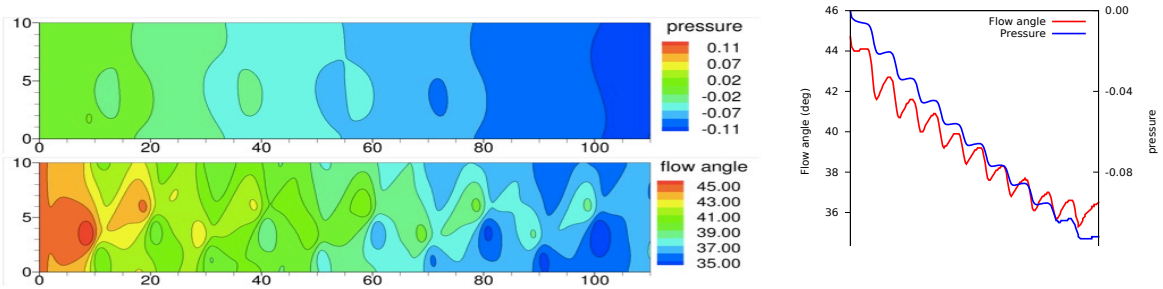

Figure 8: Pressure and flow angle: contours on the ground (left), and variation of column-averaged values with distance along the turbine row (right).

RANS simulations are also carried out for a subset of turbines in a real wind farm (located in central Iowa) for direct comparison with CWEX results. Figure 8a shows the relative locations of the meteorological towers and the turbines. The meteorological towers (shown as M1, M2, M3, & M4) in Fig. 9a are not influenced by other turbines for the wind direction shown. For purposes of comparison with data from these four towers, the rest of the turbines, which lie to the north, are ignored for the

flow directions (primarily from the south) considered here. Since there is only one column of turbines influencing the flow, the surface convergence effect is expected to be small.

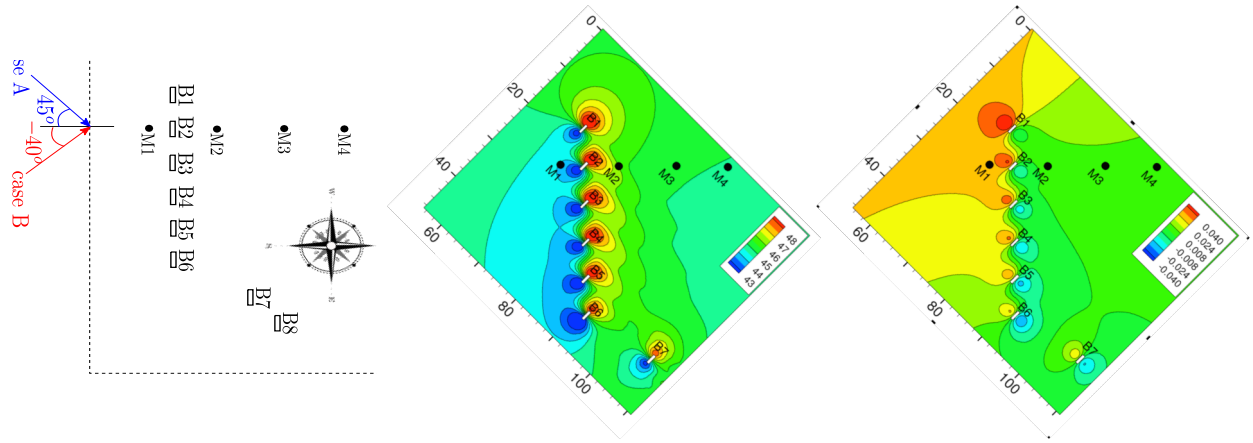

(a) (b) (c)

Figure 9: Relative locations of the meteorological towers and the turbines in the wind farm in (a). Simulations results: contours of (b) pressure and (c) flow angle, on a plane at a height of $0.27 \times r_{tip}$ above the ground for case A.

Flow angle measurements were made at the meteorological towers at a height of 0.27 × rotor radius above the ground. Flow angle is considered positive when the flow is from the southwest direction. Simulations are performed for two incoming flow angles: (case A) from southwest at 45° angle, and (case B) from southeast at 40°. The computational domain is rotated for each case such that the inlet boundary is orthogonal to the incoming flow direction to allow the use of a Dirichlet boundary condition on the side boundaries. Figure 9 plots contours of kinematic pressure and flow angle on the plane where the meteorological tower measurements were made. The projections of the turbine rotors on this plane are indicated by the hollow rectangles in these plots. Due to the large separation between turbine columns, the pressure drop and hence flow angle change is affected by only one column of turbines (denoted by B1, B2, etc.). The flow angle change measured across this column of turbines at the meteorological towers is compared with predictions in Fig. 10 for both the simulated flow angles. The vertical bars in the data show 95% confidence intervals.

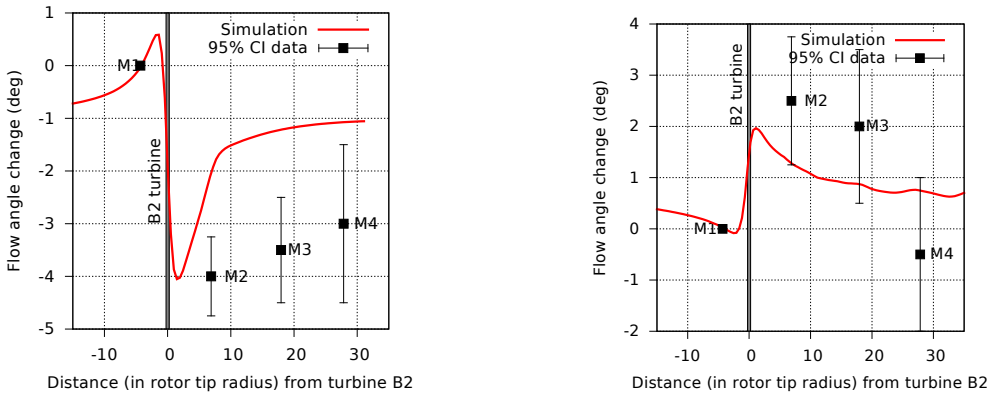

Figure 10: Change in flow angle (w.r.t. the value at M1) as functions of distance from B2 turbine for case A (left) and case B (right). In both cases a flow convergence is indicated.

The plots clearly show that both the model and measurements report the flow being rotated toward the normal to the line of turbines for both flow directions, although the measured wind rotation is larger than the rotation simulated by the model. The lower magnitude produced by the model may be due to surface friction effects (the surface vegetation was maize of height about 1.5 m) not being adequately represented in the model. However, the agreement is sufficiently close to merit further comparisons, particularly for future studies that have different surface vegetation conditions and explore the impact of multiple lines of turbines.

8. Summary

We have described a variety of experiments that are being conducted using data from Iowa meteorological towers and wind farms under CWEX. Our preliminary data reveal that conditions of high vertical shear of the horizontal wind is a common phenomenon. Analysis of turbine power production reveals that although leading turbines mostly reduce the power production of downwind turbines, there is clear evidence of turbine wakes *increasing* the power produced by downwind turbines under certain conditions. We conclude that forecasts of wind shear through 300-m is important for understanding how high speed air from above the turbines is being entrained into the turbine layer and affecting wind farm power production. Preliminary studies of surface flow convergence provide guidance for future field measurements and modeling studies of the potential mesoscale impact of wind farms.

9. Acknowledgments

Partial funding for CWEX-10 was provided by the Ames Laboratory (DOE) and the Center for Global and Regional Environmental Research at the University of Iowa. Surface flux stations for CWEX-10 were provided by the National Laboratory for Agriculture and the Environment (USDA) and for CWEX-11 were provided by NCAR Earth Observing Laboratory under an instrumentation deployment, and undergraduate student participation was supplemented by funding from an NSF REU program under grant 1063048. Data analysis was supported in part by the National Science Foundation under the State of Iowa EPSCoR Grant 1101284.

10. References

[1] IWEA 2014 Iowa Wind Energy Association [online at http://www.iowawindenergy.org/]
[2] Rajewski D A, Takle E S, Lundquist J K, Oncley S P, Prueger J H, Horst T W, Rhodes M E, Pfeiffer R, Hatfield J L, Spoth K K, and Doorenbos R K 2013 CWEX: Crop/Wind Energy Experiment: observations of surface-layer, boundary-layer and mesoscale interactions with a wind farm *Bull. Amer. Meteorol. Soc.* **94** 655
[3] Bonner W D 1968 Climatology of the low-level jet *Mon. Wea. Rev.* **96** 833
[4] Blackadar A K 1957 Boundary-layer wind maxima and their significance for the growth of nocturnal inversions *Bull. Amer. Meteorol. Soc.* **38** 283
[5] Delage Y 1974 A numerical study of the nocturnal atmospheric boundary layer *Q. J. Roy. Meteorol. Soc.* **100** 351
[6] Thorpe A J, and Guymer T H 1977 The nocturnal jet *Q. J. Roy. Meteorol. Soc.* **103** 633
[7] Zeman O 1979 Parameterization of the dynamics of stable boundary layers and nocturnal jets *J. Atmos. Sci.* **36** 792
[8] Russell R D, and Takle E S 1985 A numerical study of the effects of synoptic baroclinicity on stable boundary-layer evolution *Bound-Layer Meteor.* **31** 385
[9] Walton R A, Gallus Jr W A, and Takle E S 2013 Wind ramp events at turbine height – spatial consistency and causes at two Iowa wind farms *4th Conf on Weather, Climate and the New Energy Economy*, Austin TX Jan 6-10 P421
[10] Walton R A, Takle E S, and Gallus Jr W A 2014 Characteristics of 50-200 m winds and temperatures derived from an Iowa tall tower network, submitted to *J. Appl. Meteorol. Clim.*
[11] Courtney M, Wagner R, and Lindelow P 2008 Testing and comparison of lidars for profile and turbulence measurements in wind energy. *Proc. 14th Int. Symp. for the Advancement of Boundary Layer Remote Sensing* **1** Risø DTU, Denmark, IOP Conference Series: Earth and Environmental Science, 012021

[12] Rhodes M and Lundquist J 2013 The effect of wind turbine wakes on summertime Midwest atmospheric wind profiles *Bound.-Layer Meteorol.* **149** 85 doi:10.1007/s10546-013-9834-x
[13] Banta R M, Newsom R K, Lundquist J K,Pichugina Y L, Coulter R L, and Mahrt L 2002 Nocturnal low-level jet characteristics over Kansas during CASES-99 *Bound.-Layer Meteorol.* **105** 221
[14] Lundquist J K and Mirocha J D 2008 Interaction of Nocturnal Low-Level Jets with urban geometries as seen in Joint URBAN 2003 data *J. Appl. Meteorol. Clim.* **47** 44
[15] Wood N 2000 Wind flow over complex terrain: A historical perspective and the prospect for large-eddy modeling. *Bound.-Layer Meteor.*, **96**, 11–32.
[16] Ayotte K W, Davy R J, and Coppin P A 2001 A simple temporal and spatial analysis of flow in complex terrain in the context of wind energy modeling *Bound.-Layer Meteorol.* **98** 275
[17] Deppe A J, Gallus Jr W A, and Takle E S 2013 A WRF ensemble for improved wind speed forecasts at turbine height *Wea. Forecasting* **28** 212
[18] Hu, X-M, Klein P M, and Xue M 2013 Evaluation of the updated YSU planetary boundary layer scheme within WRF for wind resource and air quality assessments *J. Geophys. Res. Atmos.* **118** 10,490 doi:10:1002/jgrd.50823
[19] Jahn D E, Gallus Jr W A and Takle E S 2014 Evaluation of the MYNN PBL scheme closure constants for low-level jet events in a stable boundary layer *21st Symp. Bound- Layers and Turb* Amer. Meteor. Soc. Leeds UK.
[20] Francis N 2008 Predicting sudden changes in wind power generation *North American Windpower* **5** 58
[21] Greaves B, Collins J, Parkes J, and Tindal A 2009 Temporal forecast uncertainty for ramp events *Wind Engineering* **33** 309
[22] Showers Walton R, Gallus Jr W A, and Takle E S 2012 Analysis of ramp events and two-day WRF wind forecast accuracy at 80 m *Proc. 2012 Wind Energy Science, Engineering, and Policy National Science Foundation Research Experiences for Undergraduates Symposium, Ames, IA* 3/1-3/11 [Available online at http://www.meteor.iastate.edu/windresearch/resources/Binder1.pdf].
[23] Camerlin I J 2013 Meteorological phenomena impacting spatial consistency of ramp events in wind farms *Proc. 2013 Wind Energy Science, Engineering, and Policy National Science Foundation Research Experiences for Undergraduates Symposium, Ames, IA* 4/1 - 4/10. [Available online at http://www.engineering.iastate.edu/research/eri/initiatives/strategies/wei/education/]
[24] Selvaraj S, Chaves A J, Takle E S, and Sharma A 2013 Numerical prediction of flow convergence phenomenon in windfarms *Proc Conf. on Wind Energy Science and Technology*, RUZGEM 2013 October 3-4 Ankara, TURKEY.